

# The integrated bispectrum as a test of CMB non-Gaussianity: detection power and limits on $f_{NL}$ with WMAP data

P. Cabella<sup>1\*</sup>, F. K. Hansen<sup>2†</sup>, M. Liguori<sup>3,4,5‡</sup>, D. Marinucci<sup>6§</sup>, S. Matarrese<sup>4,5¶</sup>, L. Moscardini<sup>7||</sup> and N. Vittorio<sup>8,9\*\*</sup>

<sup>1</sup> *Astrophysics, University of Oxford, Denys Wilkinson Building, Keble Road, Oxford OX1 3RH, UK*

<sup>2</sup> *Institute of Theoretical Astrophysics, University of Oslo, P.O. Box 1029 Blindern, 0315 Oslo, Norway*

<sup>3</sup> *Particle Astrophysics Center, Fermi National Accelerator Laboratory, Batavia, Illinois 60510-0500, USA*

<sup>4</sup> *Dipartimento di Fisica ‘Galileo Galilei’, Università di Padova, Via Marzolo 8, I-35131 Padova, Italy*

<sup>5</sup> *INFN, Sezione di Padova, Via Marzolo 8, I-35131 Padova, Italy*

<sup>6</sup> *Dipartimento di Matematica, Università di Roma ‘Tor Vergata’, Via della Ricerca Scientifica 1, I-00133 Roma, Italy*

<sup>7</sup> *Dipartimento di Astronomia, Università di Bologna, Via Ranzani 1, I-40127 Bologna, Italy*

<sup>8</sup> *Dipartimento di Fisica, Università di Roma ‘Tor Vergata’, Via della Ricerca Scientifica 1, I-00133 Roma, Italy*

<sup>9</sup> *INFN, Sezione di Roma ‘Tor Vergata’, Via della Ricerca Scientifica 1, I-00133 Roma, Italy*

26 November 2018

## ABSTRACT

We propose a fast and efficient bispectrum statistic for Cosmic Microwave Background (CMB) temperature anisotropies to constrain the amplitude of the primordial non-Gaussian signal measured in terms of the non-linear coupling parameter  $f_{NL}$ . We show how the method can achieve a remarkable computational advantage by focussing on subsets of the multipole configurations, where the non-Gaussian signal is more concentrated. The detection power of the test, increases roughly linearly with the maximum multipole, as shown in the ideal case of an experiment without noise and gaps. The CPU-time scales as  $\ell_{\max}^3$  instead of  $\ell_{\max}^5$  for the full bispectrum which for Planck resolution  $\ell_{\max} \sim 3000$  means an improvement in speed of a factor  $10^7$  compared to the full bispectrum analysis with minor loss in precision. We find that the introduction of a galactic cut partially destroys the optimality of the configuration, which will then need to be dealt with in the future. We find for an ideal experiment with  $\ell_{\max} = 2000$  that upper limits of  $f_{NL} < 8$  can be obtained at  $1\sigma$ . For the case of the WMAP experiment, we would be able to put limits of  $|f_{NL}| < 40$  if no galactic cut were present. Using the real data with galactic cut, we obtain an estimate of  $-80 < f_{NL} < 80$  and  $-160 < f_{NL} < 160$  at 1 and  $2\sigma$  respectively.

**Key words:** cosmic microwave background - cosmology: theory - methods: numerical - methods: statistical - cosmology: observations

## 1 INTRODUCTION

In recent years a number of papers have focussed on the statistical nature of the fluctuations in the Cosmic Microwave Background radiation (CMB). In the standard inflationary scenario the quantum fluctuations of the inflaton scalar field follow a nearly Gaussian distribution, with small deviations arise by considering second-order terms of the equations (Acquaviva et al. 2003;

\* E-mail: paolo.cabella@roma2.infn.it

† E-mail: f.k.hansen@astro.uio.no

‡ E-mail: michele.liguori@pd.infn.it

§ E-mail: marinucc@mat.uniroma2.it

¶ E-mail: sabino.matarrese@pd.infn.it

|| E-mail: lauro.moscardini@unibo.it

\*\* E-mail: nicola.vittorio@roma2.infn.it

Maldacena 2003): slow-roll conditions necessarily entail that deviations from Gaussianity is very low. Nonetheless, the subsequent gravitational evolution unavoidably enhances the primordial non-Gaussian signal up to the largest scales where the primordial seeds were produced, giving rise to a non-linearity parameter (see below)  $f_{\text{NL}} \sim \mathcal{O}(1)$ . The situation changes in the presence of a second scalar field during inflation; under these circumstances it has been shown by (Bartolo Matarrese and Riotto 2002), that non-Gaussianity can be transferred from the isocurvature to the adiabatic mode, leading to non-negligible values for  $f_{\text{NL}}$  (see also (Bernardeau and Uzan; Rigopoulos, Shellard and van Tent 2005; Seery and Lidsey 2005)). Alternative scenarios for the production of the primordial seeds, such as the *curvaton* (see (Mollerach 1990; Enqvist and Sloth 2002; Lyth and Wands 2002; Moroi and Takahashi 2001; Lyth, Ungarelli and Wands 2003)) and the *inhomogeneous reheating* mechanisms (see Dvali, Gruzinov and Zaldarriaga 2004) may also lead to higher values of  $f_{\text{NL}}$ . A general review for the primordial non-Gaussian scenarios can be found in (Bartolo et al. 2004). Testing for non-Gaussianity has then become the basic tool to discriminate among different models for the production of energy-density perturbations. It has become common practice to quantify the amount of non-Gaussianity by means of the dimensionless *non-linearity parameter*  $f_{\text{NL}}$  (see, e.g. (Komatsu and Spergel 2001)), setting the strength of quadratic non-linearities in an expansion of the large-scale gravitational potential  $\Phi$  (conventionally defined so that the temperature anisotropy is  $\Delta T/T \equiv -\frac{1}{3}\Phi$  in the Sachs-Wolfe limit) in terms of a Gaussian random field  $\Phi_{\text{G}}$ , namely

$$\Phi(\mathbf{x}) = \Phi_{\text{G}}(\mathbf{x}) + f_{\text{NL}}\Phi_{\text{G}}^2(\mathbf{x}) \quad (1)$$

(up to a constant offset, which only affects the monopole contribution). Detailed calculations of the non-linearity parameter  $f_{\text{NL}}$  during and after inflation (see (Bartolo, Matarrese and Riotto 2004; Bartolo et al. 2004)) have shown that it unavoidably contains an angle-dependent part, whose role could be extremely important to look for specific signatures of inflationary non-Gaussianity as recently shown in (Liguori et al. 2005). In what follows, however, we will follow the common practice of taking  $f_{\text{NL}}$  as a constant parameter. The upper limits on the estimated value of  $f_{\text{NL}}$  have become more and more stringent as the sensitivity of CMB experiments has improved. With MAXIMA data, (Santos et al. 2003) put a limit of  $|f_{\text{NL}}| < 950$ , at  $1\sigma$  level. Using COBE data, (Komatsu et al. 2002) (with the bispectrum) and (Cayón et al. 2003) (with Spherical Mexican Hat Wavelets (SMHW)) found  $|f_{\text{NL}}| < 1500$  and  $|f_{\text{NL}}| < 1100$  respectively, at  $1\sigma$  level; these intervals were shrunk to  $-58 < f_{\text{NL}} < 134$  at  $2\sigma$  level in the first release of WMAP see (Komatsu et al. 2003). Using SMHW, (Mukherjee and Wang 2004) found  $f_{\text{NL}} = 50 \pm 80$  at  $1\sigma$  and  $f_{\text{NL}} < 220$  at  $2\sigma$  level; in (Cabella et al. 2005) we constrained  $f_{\text{NL}} = -5 \pm 175$  at  $2\sigma$  level, combining the local curvature and spherical wavelets. Very recently the constraints on  $f_{\text{NL}}$  have been improved by (Creminelli et al. 2005), who find  $-27 < f_{\text{NL}} < 121$  at  $2\sigma$  level. In (Gaztanaga and Wagg 2003) very stringent limits are found but a direct comparison with the other methods is unfeasible because of discrepancies in the non-Gaussian models adopted. In this paper we focus on functionals of the normalized bispectrum; the latter has been considered by many authors in the literature, including (Komatsu and Spergel 2001); more recently, (Babich 2005) has discussed conditions under which the bispectrum is the optimal estimator of primordial non-Gaussianity and (Babich and Zaldarriaga 2004) showed that tighter constraints are expected from a joint analysis of temperature and polarization data.

Here, we implement some procedures which were proposed in the statistical literature (Marinucci 2005). In that paper, a full analytic derivation is provided for the test behaviour in the presence of an ideal experiment; the behaviour in the presence of non-Gaussianity is also discussed. Here, we investigate the properties of these tests under a realistic experimental setting, using both simulations and WMAP data. The plan of this paper is as follows: in Section 2 we describe the proposed procedure; Section 3 and 4 describe the implementation, simulations and datasets used; Section 5 discusses the results of the procedure applied to the simulations; in Section 6 we draw some conclusions and discuss directions for future research.

## 2 THE INTEGRATED BISPECTRUM

As well-known, the angular bispectrum  $B_{l_1 l_2 l_3}^{m_1 m_2 m_3}$  is defined by

$$B_{l_1 l_2 l_3}^{m_1 m_2 m_3} = \langle a_{l_1 m_1} a_{l_2 m_2} a_{l_3 m_3} \rangle \quad (2)$$

As shown by (Hu 2001) for a statistically isotropic field it is convenient to focus on the angle-averaged bispectrum, defined by

$$B_{l_1 l_2 l_3} = \sum_{m_1=-l_1}^{l_1} \sum_{m_2=-l_2}^{l_2} \sum_{m_3=-l_3}^{l_3} \begin{pmatrix} l_1 & l_2 & l_3 \\ m_1 & m_2 & m_3 \end{pmatrix} B_{l_1 l_2 l_3}^{m_1 m_2 m_3}; \quad (3)$$

the minimum mean square error estimator is provided by

$$\widehat{B}_{l_1 l_2 l_3} = \sum_{m_1=-l_1}^{l_1} \sum_{m_2=-l_2}^{l_2} \sum_{m_3=-l_3}^{l_3} \begin{pmatrix} l_1 & l_2 & l_3 \\ m_1 & m_2 & m_3 \end{pmatrix} (a_{l_1 m_1} a_{l_2 m_2} a_{l_3 m_3}).$$

The distribution of the previous statistic depends on the angular power spectrum of the CMB. It is a standard practice to make the angular bispectrum model independent (under Gaussianity) by focussing on the normalized bispectrum, which we define by

$$I_{l_1 l_2 l_3} = (-1)^{(l_1+l_2+l_3)/2} \frac{\widehat{B}_{l_1 l_2 l_3}}{\sqrt{C_{l_1} C_{l_2} C_{l_3}}}. \quad (4)$$

The factor  $(-1)^{(l_1+l_2+l_3)/2}$  is usually not included in the definition of the normalized bispectrum; it corresponds, however, to the sign of the Wigner's coefficients for  $m_1 = m_2 = m_3 = 0$ , and thus it seems natural to include it to ensure that  $I_{l_1 l_2 l_3}$  and  $b_{l_1 l_2 l_3}$  share the same parity (see (3)). An alternative estimator of  $I_{l_1 l_2 l_3}$ , which uses the estimated rather than the theoretical bispectrum, is provided by

$$\widehat{I}_{l_1 l_2 l_3} = (-1)^{(l_1+l_2+l_3)/2} \frac{\widehat{B}_{l_1 l_2 l_3}}{\sqrt{\widehat{C}_{l_1} \widehat{C}_{l_2} \widehat{C}_{l_3}}},$$

$$\widehat{C}_l = \frac{1}{2l+1} \sum_{m=-l}^l |a_{lm}|^2$$

is the power spectrum of the given realization. In (Marinucci 2005) has shown that, under Gaussian hypothesis, the two normalizations are equivalent. A crucial issue relates to how one can combine the information from the different multipoles into a single statistic. For statistically isotropic fields the bispectrum can be non-zero only for configurations where  $l_1 + l_2 + l_3$  is even and the triangle conditions hold,  $|l_i - l_j| \leq l_k \leq l_i + l_j$ ,  $i, j, k = 1, 2, 3$ . It is not difficult to see that if we avoid repetitions there are asymptotically  $L^3/24$  such configurations, where  $L$  denotes the highest observable multipole; it is therefore computationally very hard to consider the full set of bispectrum ordinates for high resolution experiments such as WMAP or Planck. Various solutions have been considered, see for instance (Komatsu, Spergel and Wandelt 2003). In this paper, our idea is to restrict the analysis to a subset of the bispectrum ordinates where the bulk of information on non-Gaussianity is condensed.

The procedure we shall consider has been advocated in the statistical literature by (Marinucci 2005): More precisely, for finite integers  $l_0 \geq 2$ ,  $K \geq 0$  we shall consider the processes:

$$J_{L;l_0,K}(r) = \frac{1}{\sqrt{L}} \sum_{l=l_0+K+1}^{[Lr]-l_0-K} \left\{ \frac{1}{\sqrt{K+1}} \sum_{u=0}^K \widehat{I}_{l_0+u,l,l+l_0+u} \right\} \quad (5)$$

where  $[.]$  denotes the integer part of a real number;  $0 \leq r \leq 1$  and  $l_0$  is an (arbitrary but fixed) value which can be taken equal to 2 or 3, according to whether we wish to keep the quadrupole or not in the data. As usual, the sums are taken to be equal to zero when the index set is empty.  $K$  is a fixed pooling parameter: for  $K = 0$  we obtain the special case

$$J_{L;l_0}(r) = \frac{1}{\sqrt{L}} \sum_{l=l_0+1}^{[Lr]-l_0} \widehat{I}_{l_0,l,l+l_0}. \quad (6)$$

The normalizing factors are chosen to ensure an asymptotic unit variance for all summands. In words, the strategy for  $J_{L;l_0,K}(r)$  is to look at collapsed configurations; more precisely, for a fixed  $l_0$  we aim at maximizing the distance among multipoles, albeit preserving the triangle conditions  $l_i \leq l_j + l_k$ . For an ideal experiment, it is shown in (Marinucci 2005) that, as  $L \rightarrow \infty$ , for any fixed integers  $l_0 > 0$ ,  $K \geq 0$

$$J_{L;l_0,K}(r) \Rightarrow W(r), 0 \leq r \leq 1, \quad (7)$$

where  $\Rightarrow$  denotes weak convergence and  $W(r)$  standard Brownian motion, that is, the Gaussian process with zero mean, independent increments and variance  $\langle W(r)^2 \rangle = r$ . The concept of weak convergence ensures that the asymptotic distribution can be immediately derived for any continuous functional of  $J_{L;l_0,K}(r)$ ; for instance

$$\Pr \left\{ \max_{0 \leq r \leq 1} J_{L;l_0,K}(r) \geq x \right\} = 2\Phi(-x) \text{ for all } x \geq 0.,$$

where  $\Pr$  stands for the probability and  $\Phi(\cdot)$  denotes the cumulative distribution function of a standard Gaussian variate; these values are well-known and tabulated, and can be used to double-check the validity of Monte Carlo simulations.

We wish now to discuss the expected power of this procedure under simplified circumstances: we shall work in the framework of an ideal experiment and a pure Sachs-Wolfe model. The Monte Carlo evidence presented in the next section suggests, however, that our conclusions have a much more general validity. From (7) we know that, approximately

$$\text{Var} \{J_{L;l_0,K}(r)\} \sim r, \text{ for large } L;$$

also, it is well-known that the Sachs-Wolfe bispectrum can be approximated by

$$B_{l_1 l_2 l_3} = G f_{\text{NL}} h_{l_1 l_2 l_3} \begin{pmatrix} l_1 & l_2 & l_3 \\ 0 & 0 & 0 \end{pmatrix} \{C_{l_1} C_{l_2} + C_{l_2} C_{l_3} + C_{l_1} C_{l_3}\}, \quad (8)$$

where  $G$  is a positive constant,

$$h_{l_1 l_2 l_3} = \left( \frac{(2l_1 + 1)(2l_2 + 1)(2l_3 + 1)}{4\pi} \right)^{1/2},$$

and lower order terms are neglected. We shall take  $C_l \propto l^{-\alpha}$  (for some positive constant  $\alpha > 2$ ). For simplicity, let us assume that the normalizing angular power spectrum is known a priori; without loss of generality, we take  $K = 0$ . Using expressions 8.1.2.12 and 8.5.2.32 in (Varshalovich et al. 1988), it can be shown that, for fixed  $l_0 \geq 2$ ,

$$\begin{pmatrix} l_0 & l & l + l_0 \\ 0 & 0 & 0 \end{pmatrix} = C \frac{(-1)^{l_0+l}}{\sqrt{l}} + O\left(\frac{1}{l^{3/2}}\right),$$

for some  $C > 0$  which depends on  $l_0$  but not on  $l$ . Then we have easily that

$$\langle J_L(r) \rangle \propto \frac{f_{\text{NL}}}{\sqrt{L}} \sum_{l=l_0+1}^{[Lr]} \sqrt{l} \sqrt{\frac{C_{l_0} C_l}{C_{l+l_0}}} \propto f_{\text{NL}} L. \quad (9)$$

On the other hand, by a similar argument, it is easy to show that the choice of an equilateral configuration  $l_1 = l_2 = l_3 = l$  entails an asymptotic negligible power in the presence of this kind of non-Gaussianity.

The main conclusions we can draw from this heuristic discussion are as follows: ‘‘collapsed’’ configurations where the multipoles lie on the boundary of the triangle conditions seem to have an expected power of at least an order of magnitude in  $L$  larger than for configurations on the main diagonal. For a pure Sachs-Wolfe model and an ideal experiment, the signal to noise ratio is going to increase linearly for collapsed configurations, whereas no improvement is expected for equilateral configurations. It is then natural to conjecture that very little information is lost in our procedure with respect to a full analysis of all bispectrum coordinates; the latter, however, is clearly unfeasible for computational reasons, and no analytic results are available to guide the simulations. In fact whereas calculating all the elements of the bispectrum scales as  $\ell^5$  in CPU time, calculating only the collapsed configurations scales as  $\ell^3$ . With WMAP data ( $L \simeq 500$ ) we gain a factor  $10^5$  and for Planck resolution it is  $10^7$  times faster. The next section is devoted to check the validity of the above claims in a much more general and realistic setting, by means of Monte Carlo simulations.

### 3 THE AVERAGED INTEGRATED BISPECTRUM OF SIMULATED NON-GAUSSIAN MAPS

We have generated a set of 200 non-Gaussian simulations to test the power of the collapsed configurations described in the previous sections. Note that the above deductions were done for a model with fluctuations coming entirely from the Sachs-Wolfe term with no radiative transfer involved. As the analytical treatment becomes much more complex with the radiative transfer function included, we will show that the above results are still valid using simulated non-Gaussian maps. First of all, we will show that for the ‘Collapsed Configuration Bispectrum’ (CCB) signal to noise is increasing for increasing multipoles, thus making the detection probability monotonically rising with increasing angular resolution. Second, we will show that the power of the CCB is falling with increasing  $l_0$  and that all the power can be extracted using only the first few  $l_0$ . Finally, we will show that the often used diagonal configuration of the bispectrum has minimal power compared to CCB.

The non-Gaussian simulated maps were generated using the method of (Liguori, Matarrese and Moscardini 2003). We produced a set of 200 maps (unfortunately, this is very CPU demanding limiting the number of maps which can be produced), the highest multipole being  $L = 2000$  with a power spectrum similar to the best fit WMAP power spectrum (Hinshaw et al. 2003). The non-Gaussian part of the bispectrum can be obtain by making the ensemble average over 200 simulations of

$$\tilde{J}_\ell(L, L_0) \equiv \sum_{l_0=2}^{L_0} \frac{1}{\sqrt{L}} \sum_{\ell'=\ell_0+1}^{\ell} \hat{I}_{\ell_0, \ell', \ell'+\ell_0}^{\text{NG}},$$

where  $L$  is the maximum multipole used dependent on the resolution of the experiment and  $L_0$  is the maximum value of  $\ell_0$  included. Here NG means that we have only considered combinations of the type  $a_{\ell_1 m_1}^{\text{NG}} a_{\ell_2 m_2}^{\text{G}} a_{\ell_3 m_3}^{\text{G}}$  in calculating the bispectrum. Since the non-Gaussian  $a_{\ell m}^{\text{NG}}$  are many orders of magnitude smaller than the corresponding gaussian  $a_{\ell m}^{\text{G}}$  combinations with more  $a_{\ell m}^{\text{NG}}$  factors will be negligible, also confirmed by our simulations. Note that in order to normalize the  $a_{\ell m}$ , we have assumed that we are able to estimate the power spectrum well and we use the correct ensemble averaged power spectrum. In the case of cut sky and noise, this is taken into account in the normalizing power spectrum by  $C_\ell = C_\ell B_\ell^2 / f_{\text{sky}} + N_\ell$  where  $B_\ell$  is the beam,  $N_\ell$  is the noise power spectrum and  $f_{\text{sky}}$  is the sky fraction.

In figure 1, we show the  $\tilde{J}_{\ell, \ell_0}(L = 2000)$  for different  $\ell_0$ . As expected, the non-Gaussian term is monotonically increasing

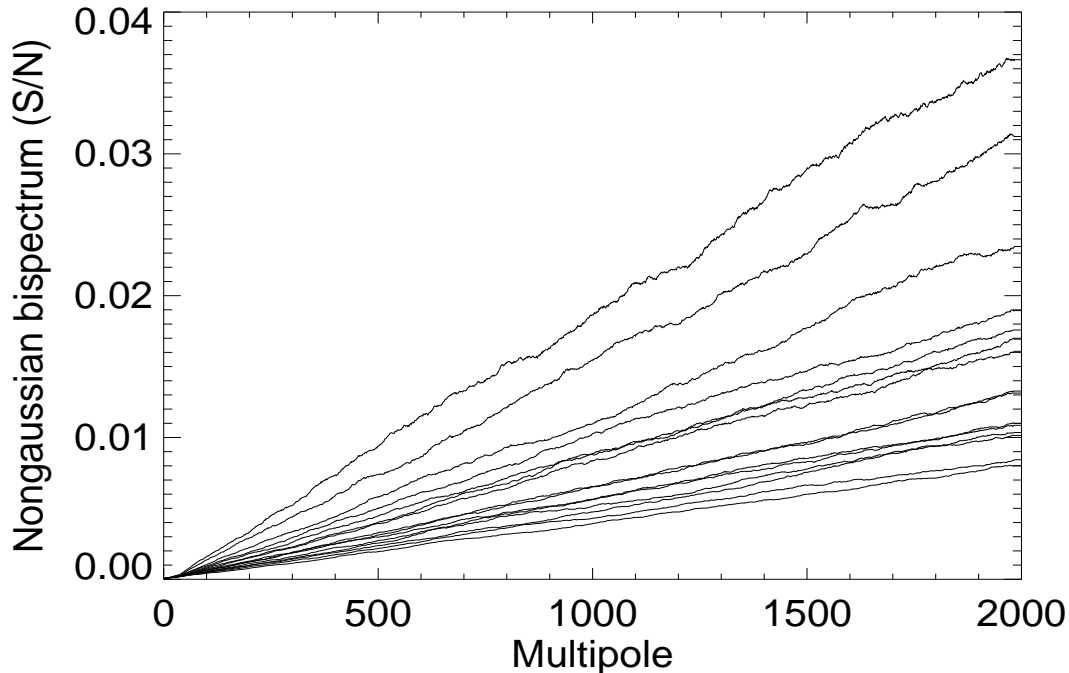


**Figure 1.** The non-Gaussian part of the integrated bispectrum (see eq. 5) averaged over 200 Monte Carlo simulations and normalized by the Gaussian standard deviation. Different values for  $\ell_0$  (with constant step  $\Delta\ell_0 = 1$ ) are shown, the lines are descending for increasing  $\ell_0$ , the highest being  $\ell_0 = 2$ , the lowest being  $\ell_0 = 16$ .

and the contribution from high  $\ell_0$  is decreasing. We also estimated the diagonal bispectrum from the same simulations and found it to be oscillating around 0, being at least three order of magnitude smaller than CCB.

#### 4 SIMULATED MAPS AND THE WMAP DATA

In the following, we will demonstrate the power of CCB on simulated maps with noise and beam specifications being those of the WMAP experiment (Bennett et al. 2003) (all data and templates are publicly available on the LAMBDA website<sup>1</sup>). Finally, we will also analyse these data and compare our results to those of (Komatsu et al. 2003) in which all elements of the bispectrum are used. We will simulate the three CMB dominated WMAP channels, the Q(41 GHz), V(61 GHz) and W(94GHz) bands, convolving with the corresponding beams and adding Gaussian noise. We will also use the Kp0 galactic cut. Note that the galactic cut may shift the optimal configurations of the bispectrum and as we will show later, using a galactic cut seems to render the CCB less optimal. All analysis will be performed on the noise-weighted linear combination of the Q, V and W channels, co-added according to (Bennett et al. 2003)

$$T_i = (T_i^Q w_Q + T_i^V w_V + T_i^W w_W) / (w_Q + w_V + w_W),$$

where  $T_i^X$  is the temperature in pixel  $i$  for channel X, and the weights are given as  $w_X = 1/\sigma_X^2$  where  $\sigma_X^2$  is the average noise variance for channel X. We will simulate 200 Gaussian realizations of CMB with the corresponding 200 non-Gaussian maps (Liguori, Matarrese and Moscardini 2003) as well as 200 independent Gaussian simulations and noise for all 400 maps to be analysed.

#### 5 ESTIMATING $f_{\text{NL}}$ IN MONTE CARLO SIMULATIONS

The scope of this section is to find the error bars on  $f_{\text{NL}}$  for the simulated WMAP data described in the previous section. These error bars will be compared to the error bars obtained by (Komatsu et al. 2003) using all elements of the bispectrum as a test of the optimality of the CCB. We will apply the full estimation procedure to maps with and without galactic cut,

<sup>1</sup> <http://lambda.gsfc.nasa.gov/>

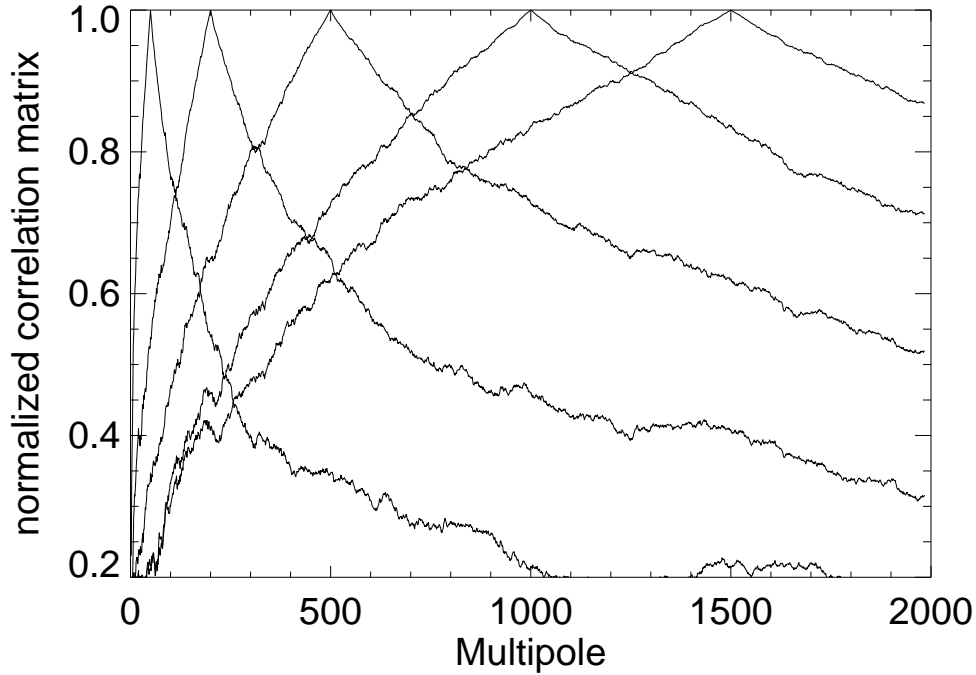


**Figure 2.** Cross sections of the normalized correlation matrix. The plot shows  $C_{\ell_0 \ell'} / \sqrt{C_{\ell_0 \ell_0} C_{\ell' \ell'}}$  for some values of  $\ell_0$ . The correlation matrix was obtained by 200 Gaussian simulations of the integrated bispectrum  $C_{\ell \ell'} = \langle \tilde{J}_\ell \tilde{J}_{\ell'} \rangle$ .

checking in this way whether introducing a sky cut causes loss of optimality (thus that the optimal configurations are shifted away from the CCB by the non-orthonormality of the spherical harmonic functions on the cut sky). Finally we will estimate  $f_{\text{NL}}$  using the real data.

In order to estimate  $f_{\text{NL}}$  from the CCB of the 200 simulated maps, we will minimize the  $\chi^2$  defined by

$$\chi^2(f_{\text{NL}}) = \mathbf{d}(f_{\text{NL}})^T \mathbf{C}^{-1} \mathbf{d}(f_{\text{NL}}),$$

with respect to  $f_{\text{NL}}$ . Here, the elements of the data vector are defined by  $d_\ell = \tilde{J}_\ell - f_{\text{NL}} * \langle \tilde{J}_\ell^{\text{NG}} \rangle$  and the correlation matrix  $C_{\ell \ell'} = \langle d_\ell d_{\ell'} \rangle - \langle d_\ell \rangle \langle d_{\ell'} \rangle$  with  $\tilde{J}_\ell$  being the 'observed' CCB. The 200 pure non-Gaussian maps are used to obtain  $\langle \tilde{J}_\ell^{\text{NG}} \rangle$ , and the 200 independent Gaussian simulations are used for obtaining the correlation matrix. Strictly speaking, the correlation matrix also depends on  $f_{\text{NL}}$  but for realistic values of  $f_{\text{NL}}$  ( $< 100$ ) this dependence is negligible. The normalized correlation matrix defined as  $\hat{C}_{\ell \ell'} \equiv C_{\ell \ell'} / \sqrt{C_{\ell \ell} C_{\ell' \ell'}}$  is shown in figure (2). The correlations between neighbouring multipoles is so strong that the matrix is numerically ill-defined. A binning procedure is necessary to enable the matrix to be inverted. Note from the figure that the long-range correlations are stronger for larger multipoles, thus a tighter binning for the lower multipoles will be allowed. We define the bin-size for a given multipole  $\ell$  following this procedure:

- define a limit  $\alpha < 1$
- start with  $\ell = 2$  and find for which  $\ell$  the value of the normalized correlation matrix  $\hat{C}_{2\ell}$  has fallen below the limit  $\alpha$ . This defines the next bin.
- Starting with the obtained multipole  $\ell'$  of the next bin, find for which multipole  $\hat{C}_{\ell' \ell}$  has fallen below the limit  $\alpha$ .
- repeat the above procedure until the highest multipole  $L$  has been reached. Check if the correlation matrix with this binning gives a numerically well defined correlation matrix. If not, repeat the above procedure with a lower limit  $\alpha$  otherwise, the binning procedure is finished and the final binning has been obtained.

Following this procedure, we obtained the binning shown in the panels of figure 3, for the different cases which we will describe in the following. Further, we estimate  $f_{\text{NL}}$  in the 200 Gaussian maps and obtain in this way the frequentist error bars. We have checked that we obtain unbiased estimates of  $f_{\text{NL}}$  and that error bars of maps with non-zero  $f_{\text{NL}}$  for realistic values ( $f_{\text{NL}} < 100$ ) do not deviate significantly from the value obtained on Gaussian realizations.

As a first test of this procedure, we estimated  $f_{\text{NL}}$  for an ideal experiment with no noise and no sky cut,  $L = 2000$  and  $L_0 = 16$ . In this case we obtained  $\Delta f_{\text{NL}} = 8$  at  $1\sigma$  being consistent with (Komatsu and Spergel 2001) who found  $\Delta f_{\text{NL}} = 3$  for an ideal experiment with  $L = 3000$  using all elements of the bispectrum.

□

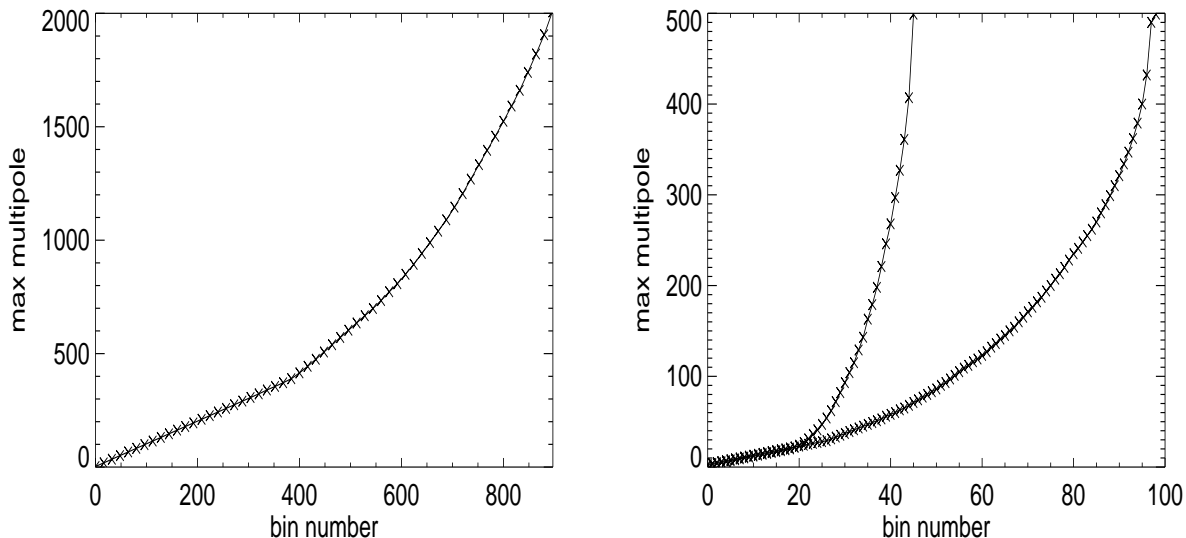


**Figure 3.** Left panel: Multipole binning for the  $\chi^2$  analysis of the high resolution simulations. On the x-axis we show the bin number and on the y-axis the corresponding last multipole of the bin. The crosses show each 16th bin to give an impression of the bin density per multipole. The limit  $\alpha$  on the correlation matrix used to construct this binning (see the text) was  $\alpha = 0.998$ . Right panel: the same, but for the WMAP simulations. The crosses are now shown for all bins. Lower line is for the case with WMAP noise but no galactic cut ( $\alpha = 0.985$ , see the text), upper line is for the case with both noise and a Kp0 cut ( $\alpha = 0.946$ )

Second, we applied the same procedure on the maps with WMAP beam and noise added (but no galactic cut) and find  $\Delta f_{\text{NL}} = 40$  which is to be compared with  $\Delta f_{\text{NL}} = 48$  obtained by (Komatsu et al. 2003) for the WMAP data. In the latter, a galactic cut of 25% (Kp0) was applied.

Finally, for the case including the Kp0 sky cut, we obtain  $\Delta f_{\text{NL}} = 80$ . Note that in this case the error has increased drastically and much more than one could expect from a simple 25% loss of data. This can be understood, looking at the right panel of figure 3 showing the binning with and without the mask. The bins are much denser without the mask, showing that the mask is introducing high correlations between multipoles. Thus the information is spread to other multipoles and the collapsed configuration is no longer optimal. This suggests to include refilling procedure in order to restore orthogonality (i.e. one could use the Gibbs sampling approach (Eriksen et al. 2004)) and just be limited by the sampling variance, this will be explored in a future work.

We have applied the procedure to the WMAP data and obtain an estimate  $f_{\text{NL}} = 0$  when sampling  $f_{\text{NL}}$  space in a grid of 10. In figure 4, we show the Gaussian standard deviation of  $\tilde{J}_\ell$  together with  $\tilde{J}_\ell$  for the WMAP data. We also show the theoretical  $\tilde{J}_\ell$  for a set of  $f_{\text{NL}}$  values. On the right panel of figure 4, we show the  $\chi^2$  around its minimum, showing that the Bayesian error bars indicate error bars of  $\Delta f_{\text{NL}}$  about 80 at  $1\sigma$  and 160 at  $2\sigma$  in agreement with the frequentist analysis.

## 6 CONCLUSIONS

The bispectrum is one of the most common statistics to test for non-Gaussianity in CMB data. In particular, for estimating the non-linear coupling constant in primordial non-Gaussian models, the bispectrum has proven to produce very stringent limits. The drawback of the bispectrum is that the number of elements scale with the maximum multipole  $L$  as  $L^3$  and computational time scales as  $L^5$ .

In this paper we have introduced a new procedure to test for non-Gaussianity on CMB data; our approach is based on an integrated form of the bispectrum, where a phase factor is introduced and the focus is narrowed on nearly-collapsed configurations. Our approach is computationally very convenient as it scales only as  $L^3$  and presents the added bonus to allow for explicit analytic results under idealized circumstances, in both Gaussian and non-Gaussian settings. The power properties are shown to be encouraging by Monte Carlo experiments: indeed some simple calculations suggest that the non-Gaussian signal grows linearly with the experiment resolution.

By comparing to limits on  $f_{\text{NL}}$  published in the literature based on all elements of the bispectrum, we have shown that the collapsed configuration bispectrum does indeed seem to produce comparable near optimal results. For the ideal experiment we can constrain  $f_{\text{NL}} < 8$  using  $L = 2000$  and for a WMAP like experiment we find  $f_{\text{NL}} < 40$  when a galactic cut is not

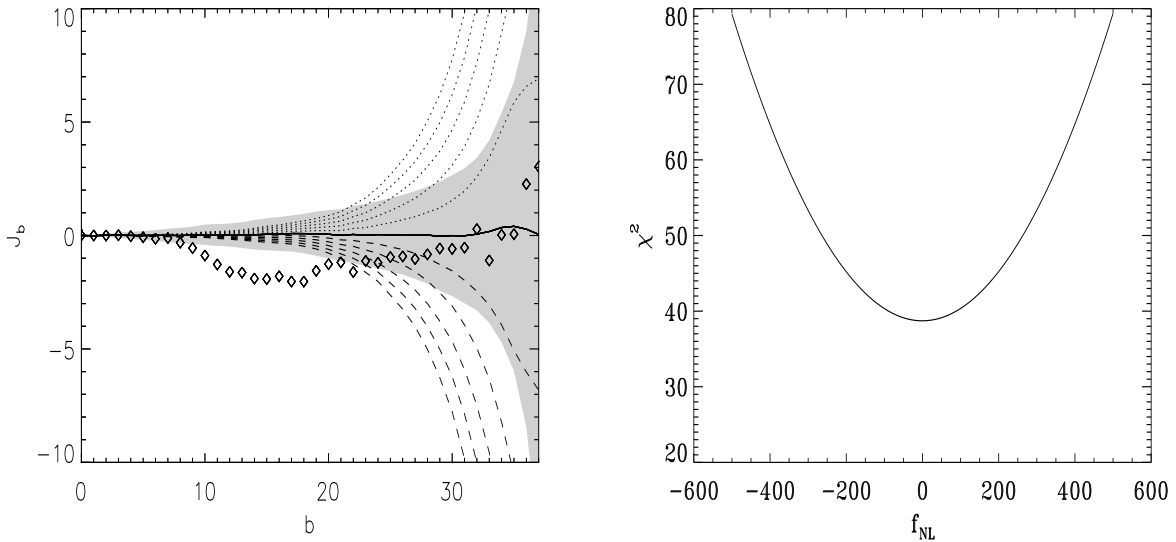


**Figure 4.** Left panel: The integrated bispectrum (see eq. 5) averaged over 200 Monte Carlo simulations with WMAP noise and Kp0 mask. The solid line represents the mean of 200 Gaussian simulations, dotted (dashed) lines represent non-Gaussian simulations for different negative (positive) values of  $f_{NL}$  from -500 to 500. The shaded area indicates the  $1\sigma$  confidence level taken from the Gaussian simulations. The diamonds show the result of WMAP data. Right panel: The  $\chi^2$  of WMAP data as a function of  $f_{NL}$ .  $f_{NL}$  is estimated to be  $0 \pm 80$  and  $0 \pm 160$  at  $1\sigma$  and  $2\sigma$  level respectively.

introduced. However, it turns out that a galactic cut does destroy the nice properties of the collapsed configuration. The multipoles get strongly coupled and the constraints on  $f_{NL}$  becomes bigger than what one would expect from a pure increase in sampling variance. For this reason, when the galactic cut is introduced, we obtain  $-80 < f_{NL} < 80$  at  $1\sigma$  applied to the WMAP data. Clearly, data from future CMB experiments like Planck will still need to be analysed with a galactic cut as it will be impossible to completely eliminate the galactic plane. For that reason, a way of dealing with the non-optimality of the collapsed configuration bispectrum will be necessary. One possible solution to this would be by some refilling procedure (or one could use the already existing Gibbs sampling technique (Eriksen et al. 2004)) which could restore orthogonality of the spherical harmonics. In this work, we did not make any prediction of the constraints on  $f_{NL}$  which can be achieved by the Planck experiment. As we are still unable to deal optimally with cut sky, this would not produce a precise limit and is therefore postponed to future work.

Finally, we note that for an ideal experiment it seems feasible to achieve the bounds predicted in (Komatsu and Spergel 2001), despite the fact that we are using here only  $L$ , rather than  $L^3$ , bispectrum configurations. On the other hand, the presence of gaps greatly deteriorated the performance of our procedure. As the collapsed bispectrum seems potentially a very promising technique for high resolution data, we view the gap handling issue as a research priority in our future work.

## ACKNOWLEDGEMENTS

We acknowledge use of the HEALPix (Górski et al. 1998) software and analysis package for deriving the results in this paper. FKH was supported by a Marie Curie reintegration grant. We acknowledge the use of the Legacy Archive for Microwave Background Data Analysis (LAMBDA). Support for LAMBDA is provided by the NASA Office of Space Science.

## REFERENCES

- Acquaviva V., Bartolo N., Matarrese S., and Riotto, 2003, Nucl. Phys. B, 667, 119  
 Babich D., 2005, Phys. Rev., D72, 043003  
 Babich D. and Zaldarriaga M., 2004, Phys. Rev., D70, 083005  
 Bartolo N., Komatsu E., Matarrese S., and Riotto N., 2004, Phys. Rep., 402, 103  
 Bartolo N., Matarrese S., and Riotto N., 2002, Phys. Rev., D65, 103505  
 Bartolo N., Matarrese S., and Riotto N., 2004, Phys. Rev. Lett., 93, 231301  
 Bennett C. L. et al., 2003, ApJS, 148, 1  
 Bernardeau F. and Uzan J. P., 2003, Phys. Rev. D67, 121301  
 Cabella P., Liguori M., Hansen F.K., Marinucci D., Matarrese S., Moscardini L., and Vittorio N., 2005, MNRAS, 358, 684



- Cayón L., Martínez-González E., Argüeso F., Banday A. J., and Górski K. M., 2003, MNRAS, 339, 1189
- Creminelli P., Nicolis A., Senatore L., Tegmark M., Zaldarriaga M., 2005, preprint (astro-ph/0509029)
- Dvali G., Gruzinov A., and Zaldarriaga M., Phys. Rev., D69, 023505
- Enqvist K. and Sloth M.S., 2002, Nucl. Phys., B 626, 395
- Eriksen H. K., O'Dwyer I. J., Jewell J. B., Wandelt B. D., Larson D. L., Gorski K. M., Levin S., Banday A. J. and Lilje P.B., 2004, ApJS, 155, 227
- Górski K. M., Hivon E. and Wandelt, B. D. 1998, Analysis Issues for Large CMB Data Sets, eds A. J. Banday, R. K. Sheth, and L. Da Costa, ESO, Printpartners Ipskamp, NL, pp.37-42
- Gaztanaga E. and Wagg J., 2003, Phys. Rev. D68, 021302
- Hinshaw G., et al. 2003, ApJS, 135, 63
- Hu W., 2001, Phys. Rev., D64, 083005
- Komatsu E., et al. 2003, ApJS, 148, 119
- Komatsu E., Wandelt B. D., Spergel D. N., Banday A. J. and Górski K. M., 2002, ApJ, 566, 19
- Komatsu E., and Spergel D.N., 2001, Phys. Rev., D63, 063002
- Komatsu, E., Spergel, D.N., and Wandelt, B.D. 2005, ApJ, 634, 14
- Liguori M., Matarrese S. and Moscardini L., 2003, ApJ., 597, 57
- Liguori M., Hansen F. K., Komatsu E., Matarrese S. and Riotto A., 2005, submitted to Phys. Rev. D, astro-ph/0509098
- Lyth D.H. and Wands D., 2002, Phys. Lett., B524, 5
- Lyth D.H., Ungarelli C., Wands D., 2003, Phys. Rev., D67, 023503
- Maldacena J. 2003, JHEP, 0305, 013
- Marinucci D., 2006, Annals of Statistics, 34, 1, preprint (math.pr/0502434)
- Mollerach S., 1990, Phys.Rev., D42, 313
- Moroi T. and Takaashi T., 2001, Phys. Lett., B522, 215 [erratum-ibid. B539 (2002) 539]
- Mukherjee P. and Wang Y., 2004, ApJ., 613, 51
- Rigopoulos G.I., Shellard E. P. S., and van Tent B W., 2005 preprint (astro-ph/0506704)
- Santos M.G., et al., 2003, MNRAS, 341, 623
- Seery D. and Lidsey J. E., 2005, JCAP 0509, 011
- Varshalovich D. A., Moskalev A.N. and Khersonskii V. K., 1988, 'Quantum theory of angular momentum', (WorldScientific Publishing)